

1
2
3 **Aliphatic Carbonyl Compounds (C₈-C₂₆) in Wintertime**
4 **Atmospheric Aerosol in London, UK**
5

6 **Ruihe Lyu^{1,2}, Mohammed Salim Alam¹, Christopher Stark¹**

7 **Ruixin Xu¹, Zongbo Shi¹, Yinchang Feng² and Roy M. Harrison^{†*1}**
8

9 **¹ Division of Environmental Health and Risk Management**
10 **School of Geography, Earth and Environmental Sciences, University of**
11 **Birmingham Edgbaston, Birmingham B15 2TT, UK**
12

13 **² State Environmental Protection Key Laboratory of Urban Ambient Air**
14 **Particulate Matter Pollution Prevention and Control, College of Environmental**
15 **Science and Engineering**
16 **Nankai University, Tianjin 300350, China**
17
18
19

20 **† Also at: Department of Environmental Sciences / Centre of Excellence in Environmental**
21 **Studies, King Abdulaziz University, PO Box 80203, Jeddah, 21589, Saudi Arabia.**
22

23 **Corresponding authors:**

24 E-mail: r.m.harrison@bham.ac.uk (Roy M. Harrison)
25

26 **ABSTRACT**

27 Three groups of aliphatic carbonyl compounds, the n-alkanals (C₈-C₂₀), n-alkan-2-ones (C₈-C₂₆) and
28 n-alkan-3-ones (C₈-C₁₉) were measured in air samples collected in London from January-April 2017.
29 Four sites were sampled including two roof-top background sites, one ground-level urban background
30 site and a street canyon location on Marylebone Road in central London. The n-alkanals showed the
31 highest concentrations followed by the n-alkan-2-ones and the n-alkan-3-ones, the latter having
32 appreciably lower concentrations. It seems likely that all compound groups have both primary and
33 secondary sources and these are considered in the light of published laboratory work on the oxidation
34 products of high molecular weight n-alkanes. All compound groups show relatively low correlation
35 with black carbon and NO_x in the background air of London, but in street canyon air heavily impacted
36 by vehicle emissions, stronger correlations emerge especially for the n-alkanals. It appears that
37 vehicle exhaust is likely to be a major contributor for concentrations of the n-alkanals whereas it is a
38 much smaller contributor to the n-alkan-2-ones and n-alkan-3-ones. Other primary sources such as
39 cooking or wood burning may be significant contributors for the ketones but were not directly
40 evaluated. It seems likely that there is also a significant contribution from photo-oxidation of n-
41 alkanes and this would be consistent with the much higher abundance of the n-alkan-2-ones relative
42 to the n-alkan-3-ones if the formation mechanism were to be through oxidation of condensed phase
43 alkanes. Vapour-particle partitioning fitted the Pankow model well for the n-alkan-2-ones but less
44 well for the other compound groups, although somewhat stronger relationships were seen at the
45 Marylebone Road site than at the background sites. The former observation gives support to the n-
46 alkane-2-ones being a predominantly secondary product, whereas primary sources of the other groups
47 are more prominent.

48 **Keywords:** Carbonyl compounds; n-alkanals; n-alkan-2-ones; n-alkan-3-ones; organic aerosol;
49 partitioning;

50 1. INTRODUCTION

51 Carbonyl compounds are classified as polar organic compounds, constituting a portion of the
52 oxygenated organic compounds in atmospheric particulate matter (PM). Aliphatic carbonyl
53 compounds are directly emitted into the atmosphere from primary biogenic and anthropogenic
54 sources (Schauer et al., 2001, 2002a, b), as well as being secondary products of atmospheric
55 oxidation of hydrocarbons (Chacon-Madrid et al., 2010; Zhang et al., 2015; Han et al., 2016).

56

57 The most abundant atmospheric carbonyls are methanal (formaldehyde) and ethanal (acetaldehyde),
58 and many studies have described their emission sources and chemical formation in urban and rural
59 samples (Duan et al., 2016). Long-chain aliphatic carbonyl compounds have been identified in PM
60 and reported in few published papers (Gogou et al., 1996; Andreou and Rapsomanikis, 2009), and
61 these compounds are considered to be formed from atmospheric oxidation processes affecting
62 biogenic emissions of alkanes. Anthropogenic activity is also considered to be a significant
63 contributor to the aliphatic carbonyls. Appreciable concentrations of aliphatic carbonyl compounds
64 have been identified in emissions from road vehicles (Schauer et al., 1999[a](#); [2002b](#)), coal combustion
65 (Oros and Simoneit, 2000), wood burning (Rogge et al., 1998) and cooking processes (Zhao et al.,
66 [2007a,b](#)), spanning a wide range of molecular weights. Furthermore, chamber studies (Chacon-
67 Madrid and Donahue, 2011; Algrim and Ziemann, 2016) have demonstrated that the aliphatic
68 carbonyl compounds are very important precursors of secondary organic aerosol (SOA) when they
69 react with OH radicals in the presence of NO_x.

70

71 The oxidation of n-alkanes by hydroxyl radical is considered to be an important source of aliphatic
72 carbonyl compounds. It was believed that the n-alkanals with carbon atoms numbering less than 20
73 indicate oxidation of alkanes, whereas the higher compounds were usually considered to be of direct
74 biogenic origin (Rogge et al., 1998). The homologues and isomers of n-alkanals and n-alkanones have
75 been identified as OH oxidation products of n-alkanes in many chamber and flow tube studies (Zhang
76 et al., 2015; Schilling Fahnstock et al., 2015; Ruehl et al., 2013; Yee et al., 2012), although not all
77 studies identified the position of the carbonyl group. The commonly accepted oxidation pathways of
78 n-alkanes generally divide into functionalization and fragmentation. Functionalization occurs when
79 an oxygenated functional group ($-\text{ONO}_2$, $-\text{OH}$, $-\text{C}=\text{O}$, $-\text{C}(\text{O})\text{O}-$ and $-\text{OOH}$) is added to a molecule,
80 leaving the carbon skeleton intact. Alternatively, fragmentation involves C–C bond cleavage and
81 produces two oxidation products with smaller carbon numbers than the reactant. The chamber studies
82 of dodecane oxidation ~~have identified 1-undecanal, hexan-3-one, octan-3-one, heptan-2-one, nonan-~~
83 ~~2-one and decan-2-one as~~ Oh include observations of aldehydes and ketones as oxidation products
84 (Schilling Fahnstock et al., 2015; Yee et al., 2012).

85

86 In London, with a high population density and a large number of diesel engine vehicles, the aliphatic
87 hydrocarbons constitute an important fraction of ambient aerosols. Anthropogenic activities and
88 secondary formation ~~favour~~ contribute to the emission and production of carbonyl compounds within
89 the city. The objectives of the present study were the identification and quantification of aliphatic
90 carbonyl compounds in particle and vapour samples collected in London from January to April 2017.
91 This work has aided an understanding of the concentrations and secondary formation of carbonyls in
92 the London atmosphere. Spatial and temporal variations of the studied carbonyl compounds were

93 assessed and used to infer sources. One of the main objectives was to provide gas/particle partitioning
94 coefficients of identified carbonyls under realistic conditions. Diagnostic criteria were used to
95 estimate the sources of identifiable atmospheric carbonyl compounds. Additionally, for the first time,
96 concentrations of particulate and gaseous n-alkan-3-ones are reported.

97

98 **2. MATERIALS AND METHODS**

99 **2.1 Sampling Method and Site Characteristics**

100 Three sampling campaigns were carried out between 23 January and 18 April 2017 at four sampling
101 sites (Figure 1) in London. The first campaign used two sampling sites, one located on the roof of a
102 building (15 m above ground) of the Regent's University (51°31'N, -0°9'W), hereafter referred to as
103 RU, sampled from 23 January 2017 to 19 February 2017, the other located on the roof (20 m above
104 ground) of a building which belongs to the University of Westminster on the southern side of
105 Marylebone Road (hereafter referred to as WM), sampled from 24 January 2017 to 20 February 2017.
106 The third sampling site was located at ground level at Eltham (51°27'N, 0°4'E), hereafter referred to
107 as EL, sampled from 23 February 2017 to 21 March 2017, which is located in suburban south London,
108 and the fourth sampling site was located at ground level on the southern side of Marylebone Road
109 (51°31'N, -0°9'W), hereafter referred to as MR, sampled from 22 March 2017 to 18 April 2017.
110 Marylebone Road is in London's commercial centre, and is an important thoroughfare carrying 80-
111 90,000 vehicles per day through central London. The Regent's University site is within Regent's
112 Park to the north of Marylebone Road. The Eltham site is in a typical residential neighbourhood, 22
113 km from the MR site. Earlier work at the Marylebone Road and a separate Regent's Park site is
114 described by Harrison et al. (2012).

115

116 The particle samples were collected on polypropylene backed PTFE filters (47 mm, Whatman) which
117 preceded stainless steel sorbent tubes packed with 1cm quartz wool, 300 mg Carbograph 2TD 40/60
118 (Markes International, Llantrisant, UK) and sealed with stainless-steel caps before and after sampling.
119 Sampling took place for sequential 24-hour periods at a flow rate of 1.5 L min⁻¹ using an in-house
120 developed automated sampler. Field blank filters and ~~adsorption-sorbent~~ tubes were prepared for
121 each site, and recovery efficiencies were evaluated. After the sampling, each filter was placed in a
122 clean sealed petri dish, wrapped in aluminium foil and stored in the freezer at -18°C prior to analysis.
123 Black carbon (BC) was simultaneously monitored during the sampling period at RU and WM sites
124 using an aethalometer (Model AE22, Magee Science). Measurements of BC and NO_x at MR and
125 NO_x at EL were provided by the national network sites of Marylebone Road, and Eltham ([https://uk-
126 air.defra.gov.uk/](https://uk-air.defra.gov.uk/)).

127

128 **2.2 Analytical Instrumentation**

129 The particle samples were analyzed using a 2D gas chromatograph (GC, 7890A, Agilent
130 Technologies, Wilmington, DE, USA) equipped with a Zoex ZX2 cryogenic modulator (Houston,
131 TX, USA). The first dimension was equipped with a SGE DBX5, non-polar capillary column (30.0
132 m, 0.25 mm ID, 0.25 mm – 5.00% phenyl polysilphenylene-siloxane), and the second-dimension
133 column equipped with a SGE DBX50 (4.00 m, 0.10 mm ID, 0.10 mm – 50.0% phenyl
134 polysilphenylene-siloxane). The GC × GC was interfaced with a Bench-ToF-Select, time-of-flight
135 mass spectrometer (ToF-MS, Markes International, Llantrisant, UK). The acquisition speed was 50.0

136 Hz with a mass resolution of >1200 fwhm at 70.0 eV and the mass range was 35.0 to 600 m/z. All
137 data produced were processed using GC Image v2.5 (Zoex Corporation, Houston, US).

138

139 **2.3 Analysis of Samples**

140 Standards used in these experiments included 19 alkanes, C₈ to C₂₆ (Sigma-Aldrich, UK, purity
141 >99.2%); 12 n-aldehydes, C₈ to C₁₃ (Sigma-Aldrich, UK, purity ≥95.0%), C₁₄ to C₁₈ (Tokyo
142 Chemical Industry UK Ltd, purity >95.0%); and 10 2-ketones, C₈ to C₁₃ and C₁₅ to C₁₈ (Sigma-
143 Aldrich, UK, purity ≥98.0%) and C₁₄ (Tokyo Chemical Industry UK Ltd, purity 97.0%).

144

145 The filters were spiked with 30.0 µL of 30.0 µg mL⁻¹ deuterated internal standards (dodecane-d₂₆,
146 pentadecane-d₃₂, eicosane-d₄₂, pentacosane-d₅₂, triacontane-d₆₂, butylbenzene-d₁₄, nonylbenzene-
147 2,3,4,5,6-d₅, biphenyl-d₁₀, p-terphenyl-d₁₄; Sigma-Aldrich, UK) for quantification and then
148 immersed in dichloromethane (DCM), and ultra-sonicated for 20.0 min at 20.0°C. The extract was
149 filtered using a clean glass pipette column packed with glass wool and anhydrous Na₂SO₄, and
150 concentrated to 50.0 µL under a gentle flow of nitrogen for analysis using GC × GC-ToF-MS. 1 µL
151 of the extracted sample was injected in a split ratio 100:1 at 300°C. The initial temperature of the
152 primary oven (80.0°C) was held for 2.0 min and then increased at 2.0 °C min⁻¹ to 210°C, followed by
153 1.5 °C min⁻¹ to 325 °C. The initial temperature of the secondary oven (120°C) was held for 2.0 min
154 and then increased at 3.0°C min⁻¹ to 200°C, followed by 2.00°C min⁻¹ to 300°C and a final increase
155 of 1.0°C min⁻¹ to 330 °C to ensure all species passed through the column. The transfer line
156 temperature was 330 °C and the ion source temperature was 280°C. Helium was used as the carrier

157 gas at a constant flow rate of 1.0 mL min⁻¹. Further details of the instrumentation and data processing
158 methods is given by Alam et al. (2016a,b).

159

160 The sorbent tubes were analyzed by an injection port thermal desorption unit (Unity 2, Markes
161 International, Llantrisant, UK) and subsequently analyzed using GC × GC-ToF-MS. Briefly, the
162 tubes were spiked with 1 ng of deuterated internal standard for quantification and desorbed onto the
163 cold trap at 350°C for 15.0 min (trap held at 20.0°C). The trap was then purged onto the column in
164 a split ratio of 100:1 at 350°C and held for 4.0 min. The initial temperature of the primary oven
165 (90.0°C) was held for 2.0 min and then increased to 2.0°C min⁻¹ to 240°C, followed by 3.0°C min⁻¹
166 to 310°C and held for 5.0 min. The initial temperature of the secondary oven (40.0°C) was held for
167 2.0 min and then increased at 3.0°C min⁻¹ to 250°C, followed by an increase of 1.5°C min⁻¹ to 315°C
168 and held for 5.0 min. Helium was used as carrier gas for the thermally desorbed organic compounds,
169 with a gas flow rate of 1.0 mL min⁻¹.

170

171 *Qualitative analysis*

172 Compound identification was based on the GC×GC-TOFMS spectra library, NIST mass spectral
173 library and in conjunction with authentic standards. Compounds within the homologous series for
174 which standards were not available were identified by comparing their retention time interval between
175 their homologues, and by comparison of mass spectra to the standards for similar compounds within
176 the series, by comparison to the NIST mass spectral library and by the analysis of fragmentation
177 patterns.

178

179 *Quantitative analysis*

180 An internal standard solution (~~including dodecane d₂₆, pentadecane d₃₂, eicosane d₄₂, pentacosane~~
181 ~~d₅₂, triacontane d₆₂, nonylbenzene 2,3,4,5,6-d₅, butylbenzene d₁₄, biphenyl d₁₀, p-terphenyl d₁₄)~~
182 ~~(Sigma-Aldrich, UK outlined above)~~ was added to the samples to extract prior to instrumental analysis.

183 Five internal standards (pentadecane-d₃₂, eicosane-d₄₂, pentacosane-d₅₂, triacontane-d₆₂,
184 nonylbenzene-2,3,4,5,6-d₅) were used in the calculation of carbonyl compound concentrations.

185

186 The quantification for alkanes, aldehydes and 2-ketones was performed by the linear regression
187 method using seven-point calibration curves (0.05, 0.10, 0.25, 0.50, 1.00, 2.00, 3.00 ng μL^{-1})
188 established between the authentic standards/internal standard concentration ratios and the
189 corresponding peak area ratios. The calibration curves for all target compounds were highly linear
190 ($r^2 > 0.99$, from 0.990 to 0.997), demonstrating the consistency and reproducibility of this method.

191 Limits of detection for individual compounds were typically in the range 0.04–0.12 ng m^{-3} . 3-ketones
192 were quantified using the calibration curves for 2-ketones. This applicability of quantification of
193 individual compounds using isomers of the same compound functionality (which have authentic
194 standards) has been discussed elsewhere and has a reported uncertainty of 24% (Alam et al., 2018).

195 Alkan-2-ones and alkan-3-ones were not well separated by the chromatography. These were separated
196 manually using the peak cutting tool, attributing fragments at m/z 58 and 71 to 2-ketones and m/z 72
197 and 85 to 3-ketones. ~~The calibration for 2 ketones was applied to quantification of the 3 ketones.~~

198 Field and laboratory blanks were routinely analysed to evaluate analytical bias and precision. Blank
199 levels of individual analytes were normally very low and in most cases not detectable. Recovery
200 efficiencies were determined by analyzing the blank samples spiked with standard compounds. Mean

201 recoveries ranged between 78.0 and 102%. All quantities reported here have been corrected according
202 to their recovery efficiencies.

203

204 3. RESULTS AND DISCUSSION

205 3.1 Mass Concentration of Particle-Bound Carbonyl Compounds

206 The study of temporal and spatial variations of air pollutants can provide valuable information about
207 their sources and atmospheric processing. The time series of particle-bound n-alkanals, n-alkan-2-
208 ones, and n-alkan-3-ones are plotted in Figure- 32. It is clear that the concentrations of n-alkanals
209 varied substantially with date, and were always higher than n-alkanones at four sites. It is also clear
210 from Figure 23 that concentrations were broadly similar at the background sites, RU, WM and EL,
211 but are elevated, especially for the n-alkanals, at MR. This is strongly indicative of a road traffic
212 source.

213

214 Carbonyls including n-alkan-2-one and n-alkan-3-one homologues could result as fragmentation
215 products from larger alkane precursors during gas-phase oxidation (Yee et al., 2012; Schilling
216 Fahnestock et al., 2015) or as functionalized products from heterogeneous oxidation of particle-bound
217 alkanes (Ruehl et al., 2013; Zhang et al., 2015). While carbonyl compounds are expected to be
218 amongst first generation oxidation products of alkanes, product yields are not well known, and are
219 highly dependent upon the chemical environment in which oxidation occurs. Yee et al. (2012) show
220 substantial yields of mono-carbonyl product, the position of substitution undefined, in the low-NO_x
221 oxidation of n-dodecane. Ruehl et al. (2013) report the production of 2- through 14-octacosanone

222 from the oxidation of octacosane, giving relative, but not absolute yields. Schilling Fahnestock et
223 al. (2014) report oxidation products of dodecane formed in both low-NO and high NO environments
224 (<d.l and NO = 97.5 ppb respectively). A singly substituted unfragmented ketone product is
225 reported only from the low-NO oxidation, and in relatively low yield amongst many products. Lim
226 and Ziemann (2009) propose a reaction scheme for the OH-initiated oxidation of alkanes in the
227 presence of NO_x. They express the view that first generation carbonyl formation is negligible at
228 high NO concentrations for linear alkanes with C_n>6 since reactions of an alkylperoxy radical with
229 O₂ are too slow to compete with isomerisation, which leads ultimately to hydroxynitrate and
230 hydroxycarbonyl products. Ziemann (2011) also shows a substantial yield of alkylnitrates from OH-
231 initiated oxidation of n-alkanes from C₁₀-C₂₅ in the presence of NO. The NO concentrations in the
232 background air of London are <12 ppb typically (UK-Air, 2018), and hence lie between the low and
233 high NO environments of experiments in the literature, therefore most probably permitting some
234 oxidation to proceed through pathways leading to first generation carbonyl products.

235

236 Figure- 2-3 shows the average total concentrations of particle-bound 1-alkanals, n-alkan-2-ones, and
237 n-alkan-3-ones from January to April at four measurement sites, and the particle and gaseous phase
238 concentrations are detailed in the Table S1 (Supporting Information). Total n-alkanals was defined
239 as the sum of particle-bound n-alkanals ranging from C₈ to C₂₀. The particulate n-alkanals at the MR
240 site accounted for 75.2% of the measured particle carbonyls with the average total concentration of
241 682 ng m⁻³, and concentrations at the other sites were 167 ng m⁻³ at EL, 117 ng m⁻³ at WM and 82.6
242 ng m⁻³ at RU, accounting for 57.0%, 57.9% and 56.3% of the measured particulate carbonyls,
243 respectively. The n-alkanals identified in this study differed ~~in some aspects~~ substantially from those

244 previously reported in samples collected from Crete (Gogou et al., 1996) and Athens (Andreou and
245 Rapsomanikis, 2009) in Greece. The n-alkanals from London presented narrower ranges of carbon
246 numbers and a higher concentration than rural and urban samples from Crete. The concentrations of
247 n-alkanal homologues (C₈-C₂₀) ranged from 5.50 to 141 ng m⁻³ (average 52.0 ng m⁻³) at MR which
248 were far higher than 1.48-28.6 ng m⁻³ (average 6.44 ng m⁻³) at RU, 1.42-50.3 ng m⁻³ (average 9.03
249 ng m⁻³) at WM and 3.29-53.0 ng m⁻³ (average 13.0 ng m⁻³) at EL (Table S1), unlike Crete where the
250 concentrations were 0.9-3.7 ng m⁻³ in rural (C₁₅-C₃₀) and 5.4-6.7 ng m⁻³ in urban (C₉-C₂₂) samples,
251 and the average concentration of all four sites was much higher than the 0.91 ng m⁻³ measured in
252 Athens (Andreou and Rapsomanikis, 2009) (C₁₃-C₂₀). This is a clear indication of a road traffic,
253 most probably diesel source which is greater in London.

254
255 As part of the CARBOSOL project (Oliveira et al., 2007), air samples were collected in summer and
256 winter at six rural sites across Europe. The particulate n-alkanals ranged from C₁₁ to C₃₀ with average
257 total concentrations between 1.0 ng m⁻³ and 19.0 ng m⁻³, with higher concentrations in summer than
258 winter at all but one site. ~~These concentrations fall well below those measured in the present study,~~
259 ~~although the range of compounds differed.~~ Maximum concentrations at all sites were in
260 compounds >C₂₂ indicating a source from leaf surface abrasion products and biomass burning
261 (Simoneit et al., 1967; Gogou et al., 1996). This far exceeds the C_{max} values seen in the particulate
262 fraction at our sites.

263
264 Atmospheric concentrations of long-chain n-alkan-3-ones have not previously been reported in the
265 literature. The n-alkan-2-one and n-alkan-3-one homologues with few carbon atoms are believed

266 mainly to originate as the fragmental products of n-alkanes (Yee et al., 2012; Schilling Fahnstock
267 et al., 2015), whereas the higher compounds are mainly generated from functional pathways (Zhang
268 et al., 2015; Ruehl et al., 2013).

270 The n-alkan-2-one homologues measured in London ranged from C₈ to C₂₆, and the average total
271 particulate fraction concentration was 58.5 ng m⁻³ at RU, 75.1 ng m⁻³ at WM, 112 ng m⁻³ at EL and
272 186 ng m⁻³ at MR, approximately accounting for 39.9% (RU), 37.0% (WM), 38.1% (EL) and 20.5%
273 (MR) of the total particulate carbonyls, respectively (Figure- 23). The published data from Greece
274 indicated that the concentrations of n-alkan-2-ones were independent of the seasons, and an average
275 of 5.40 ng m⁻³ (C₁₃-C₂₉) was measured in August and 5.44 ng m⁻³ in March at Athinas St, but 12.88
276 ng m⁻³ was measured in March at the elevated (20 m) AEDA site in Athens (Gogou et al., (1996).
277 Concentrations in Crete for alkan-2-ones (C₁₀-C₃₁) were 0.4-2.1 ng m⁻³ at the rural site and 1.9-2.6
278 ng m⁻³ at the urban site (Andreou and Rapsomanikis, 2009). The CARBOSOL project also
279 determined concentrations of n-alkan-2-ones, between C₁₄ and C₃₁ with a C_{max} at C₂₈ or C₂₉ at all
280 but one site. Average concentrations ranged from 0.15 ng m⁻³ (C₁₇₋₂₉) to 3.35 (C₁₄-C₃₁), very much
281 below the concentrations at our London sampling site. Cheng et al. (2006) measured concentrations
282 of n-alkan-2-ones in the Lower Fraser Valley, Canada, in PM_{2.5}. Samples collected in a road tunnel
283 showed the highest concentrations, total 1.8-12.6 ng m⁻³ for C₁₀-C₃₁, and were higher in daytime
284 than nighttime. Concentrations at a forest site were 1.1-7.2 ng m⁻³ without a diurnal pattern. Values
285 of C_{max} ranged from C₁₆₋₁₇ at the road tunnel to C₂₇ (secondary maximum) at the forest site. Values
286 of CPI averaged across sites from 1.00 to 1.34, giving little evidence for a substantial biogenic input

287 from higher plant waxes. These data clearly suggest a road traffic source in London, but less
288 influential than for the n-alkanals for which the increment at the roadside MR site is much greater.

289

290 ~~Atmospheric concentrations of long chain n-alkan-3-ones have not previously been reported in the~~
291 ~~literature. The n-alkan-2-one and n-alkan-3-one homologues with few carbon atoms are believed~~
292 ~~mainly to originate as the fragmental products of n-alkanes (Yee et al., 2012; Schilling Fehnestock~~
293 ~~et al., 2015), whereas the higher compounds are mainly generated from functional pathways (Zhang~~
294 ~~et al., 2015; Ruehl et al., 2013).~~ The n-alkan-3-one homologues identified in the samples ranged
295 from C₈ to C₁₉, and the average of individual compound concentrations was 0.52 ng m⁻³ at RU, 0.94
296 ng m⁻³ at WM, 1.37 ng m⁻³ at EL and 3.34 ng m⁻³ at MR. The concentrations of n-alkan-3-ones at
297 the four sites were lower than the n-alkanals and n-alkan-2-ones, and MR had the highest average
298 total mass concentrations 39.4 ng m⁻³, followed by 14.3 ng m⁻³ at EL, 10.4 ng m⁻³ at WM and 5.65
299 ng m⁻³ at RU, respectively.

300

301 The isomeric carbonyls formed via OH-initiated heterogeneous reactions of n-octacosane (C₂₈)
302 exhibit a pronounced preference at the 2-position of the molecule chain (Ruehl et al., 2013). The n-
303 octacosan-2-ones have the highest relative yield (1.00), followed by n-octacosan-3-ones (0.50), while
304 other isomeric carbonyl yields were lower than 0.20. The same results were found in the subsequent
305 chamber studies of n-alkanes (Zhang et al., 2015) (C₂₀, C₂₂, C₂₄ but not C₁₈). The main probable
306 reason was that a large fraction of C₁₈ evaporated into the gas phase, and OH oxidation happened in
307 the gas phase (homogeneous reaction). This may be supported by the evidence from previous studies
308 (Kwok and Atkinson, 1995; Ruehl et al., 2013), which found that the isomeric distribution of

309 oxidation products of n-alkanes depends upon whether the reaction occurs in the gas phase or at the
310 particle surface (Kwok and Atkinson, 1995; Ruehl et al., 2013). The homogeneous gas-phase
311 oxidation occurs fast, and H-abstraction by OH radicals occurs at all carbon sites. The fractions of
312 the OH radical reaction by H atom abstraction from n-decane at the 1-, 2-, 3-, 4- and 5-positions are
313 3.10%, 20.7%, 25.4%, 25.4%, and 25.4%, respectively, and the products from gas phase
314 (homogeneous) reaction were generally in accord with structure-reactivity relationship (SRR)
315 predictions (Kwok and Atkinson, 1995; Aschmann et al., 2001). Zhang et al. (2015) report on the
316 competition between homogeneous and heterogeneous oxidation of medium to high molecular weight
317 alkanes. They express the view that in the atmosphere, compounds typically classified as semi-
318 volatile evaporate sufficiently rapidly that homogeneous gas phase oxidation is more rapid than
319 oxidation in the condensed phase. Recently published studies have found that the isomeric
320 distribution of first-generation oxidation products of n-alkanes depends strongly upon whether the
321 reaction occurs in the gas phase or at the particle surface (Kwok and Atkinson, 1995; Ruehl et al.,
322 2013). The homogeneous gas phase oxidation occurs fast, and H abstraction by OH radicals occurs
323 at all carbon sites. The fractions of the OH radical reaction by H atom abstraction from n-decane at
324 the 1-, 2-, 3-, 4- and 5-positions are 3.10%, 20.7%, 25.4%, 25.4%, and 25.4%, respectively, and the
325 products from homogeneous reaction were generally in accord with structure-reactivity relationship
326 (SRR) predictions (Kwok and Atkinson, 1995; Aschmann et al., 2001). Reaction of particulate n-
327 alkanes is dominated by heterogeneous reactions with OH, and the H abstraction occurs preferentially
328 at the 2-position of the carbon chain (Zhang et al., 2015; Ruehl et al., 2013). The n-alkanes diffuse
329 from the inner particle to the surface, where the OH will quickly attack the H atom of 1 and 2 position
330 carbons. The intermediate products at the 2-position are relatively more stable than at the 1-position,

331 ~~and the products are dominated by oxidation of the 2-position. The isomeric carbonyls formed via~~
332 ~~OH initiated heterogeneous reactions of n-octacosane (C₂₈) exhibit a pronounced preference at the 2-~~
333 ~~position of the molecule chain¹⁸. The n-octacosan 2-ones have the highest relative yield (1.00),~~
334 ~~followed by n-octacosan 3-ones (0.50), while other isomeric carbonyl yields were lower than 0.20.~~
335 ~~The same results were found in the subsequent chamber studies of n-alkanes (Zhang et al., 2015) (C₂₀,~~
336 ~~C₂₂, C₂₄) but not C₁₈. The main reason was that OH oxidation of C₁₈ was dominated by the~~
337 ~~homogeneous reaction as a large fraction of C₁₈ evaporated into the gas phase.—~~

338

339 During the field experiment, the n-alkanal homologues were abundant in all samples, and this is
340 probably attributable to the primary emission sources, including diesel vehicles (Schauer et al.,
341 1999a), gasoline cars (Schauer et al., 2002b), wood burning (Rogge et al., 1998) and cooking aerosol
342 (Schauer et al., 1999b). Correlations with other largely vehicle-generated pollutants (see later)
343 support this interpretation. ~~During the field experiment, the 1-alkanal homologues were abundant~~
344 ~~in all samples, and this could be explained by a strong impact of anthropogenic activities. Thus, the~~
345 ~~n-alkanals are considered to arise mainly from primary emission sources. Furthermore, t~~
346 ~~particulate form of the n-alkane homologues (C₁₄-C₃₆) identified in the samples ranged from 50-~~
347 ~~100% dominated for >C₂₅ in contrast to and there was a significant particulate fraction for all but the~~
348 ~~low MW n-alkanes (unpublished data C₁₁-C₁₃). The H-abstraction by OH radicals may therefore have~~
349 ~~been dominated by heterogeneous reactions generating the higher concentrations of n-alkan-2-ones~~
350 ~~than n-alkan-3-ones that were found in all samples. The ratio of n-alkan-2-ones/n-alkan-3-ones (C₁₁-~~
351 ~~C₁₈) with the same carbon atom number ranged from 2.35-11.3 at four measurement sites.~~
352 ~~Surprisingly, although the n-alkane (C₁₁-C₁₃) oxidation was expected to be dominated by~~

353 homogeneous gas phase reactions, the n-alkan-2-one/n-alkan-3-one ratios were still greater than 2.00.
354 The probable reason was that the lower molecular weight n-alkan-2-ones were significantly impacted
355 by primary emission sources such as cooking (Zhao et al., 2007a,b). Another likely reason is that the
356 n-alkan-2-one and n-alkan-3-one homologues with lower carbon atom numbers originated in part
357 from the fragmental products of higher n-alkanes (Yee et al., 2012; Schilling Fahnstock et al., 2015).
358
359 The ratios of n-alkan-2-ones/n-alkanes, n-alkan-3-ones/n-alkanes (with same carbon numbers) were
360 calculated and are reported in Table S2. The n-alkan-3-ones with carbon numbers higher than C₂₀
361 were not identified in the samples, indicating that both the homogeneous gas phase and heterogeneous
362 reactions of higher molecular weight n-alkanes were slow, the former probably due to the low vapour
363 phase presence of n-alkanes. The ratios of n-alkan-3-ones/n-alkanes at four measurement sites
364 gradually increased from C₁₁, and then decreased from C₁₇, while higher ratios of n-alkan-2-ones/n-
365 alkanes were observed in the range from C₁₇ to C₂₂, probably indicating a shift from homogeneous
366 reactions to heterogeneous reactions with the increase of carbon numbers. The low ratios of n-alkan-
367 2-ones/n-alkanes with carbon numbers from C₂₃ to C₂₆ ~~were attributed to~~ might be explained by the
368 low diffusion rate from the inner particle to the surface with the increasing carbon number of n-
369 alkanes, even though heterogeneous reactions ~~were~~ would be the expected dominant pathway.

370

371 **3.2 Temporal and Spatial Variations**

372 ~~The study of temporal and spatial variations of air pollutants can provide valuable information about~~
373 ~~their sources and atmospheric processing. The time series of particle-bound n-alkanals, n-alkan-2-~~
374 ~~ones, and n-alkan-3-ones are plotted in Fig. 3. It is clear that the concentrations of n-alkanals varied~~

375 ~~substantially with date, and were always higher than n-alkanones at four sites. It is also clear from~~
376 ~~Figure 2 that concentrations were broadly similar at the background sites, RU, WM and EL, but are~~
377 ~~elevated, especially for the n-alkanals, at MR. This is strongly indicative of a road traffic source.~~

378

379 **3.3.2 Sources of Carbonyl Compounds**

380 **3.3.2.1 Homologue distribution and carbon preference index (CPI)**

381 ~~Figure-~~ 4 shows the average concentrations, and molecular distributions of particle-bound carbonyl
382 compounds at the four sites. The values of carbon preference index (CPI) were calculated to estimate
383 the origin of carbonyl compounds, according to Bray and Evans (1961):

384

$$385 \text{ CPI} = \frac{1}{2} \left(\frac{\sum_4^m C_{2i+1}}{\sum_4^m C_{2i}} + \frac{\sum_4^m C_{2i+1}}{\sum_5^{m+1} C_{2i}} \right)$$

$$386 \text{ For n-alkanals and n-alkan-3-ones (m=9): CPI} = \frac{1}{2} \left(\frac{\sum \text{odd}(C_9-C_{19})}{\sum \text{even}(C_8-C_{18})} + \frac{\sum \text{odd}(C_9-C_{19})}{\sum \text{even}(C_{10}-C_{20})} \right)$$

$$387 \text{ For n-alkan-2-ones (m=12): CPI} = \frac{1}{2} \left(\frac{\sum \text{odd}(C_9-C_{25})}{\sum \text{even}(C_8-C_{24})} + \frac{\sum \text{odd}(C_9-C_{25})}{\sum \text{even}(C_{10}-C_{26})} \right)$$

388

389 where i takes values between 4 and m , and 5 and m as in the equation, and

390 $m = 9$ for n-alkanal and n-alkan-3-ones

391 $m = 12$ for n-alkan-2-ones

392

393 The carbon ~~maximum~~ number of the homologue of highest concentration (C_{\max}) ~~was used to evaluate~~
394 ~~the relative contribution can be indicative~~ of the source, ~~and exhibit the homologue distribution of~~

395 ~~highest concentration.~~ Table. 1 presents the CPI and C_{\max} of particle-bound carbonyl compounds
396 calculated in the current and other studies. A CPI of ≤ 1 is an indication of an anthropogenic source,
397 while a CPI of 1-5 shows a mixture of anthropogenic and biogenic sources and a CPI >5 suggests a
398 biogenic (plant wax) source.

399
400 The n-alkanes which are potential precursors of the oxygenates described typically showed two C_{\max}
401 values, the first at C_{13} (the lowest MW compound measured), and at C_{23} . The CPI values for the
402 n-alkanes were between 0.97-1.02 at the four measurements sites (unpublished data).

403
404 According to the low CPI (0.41-1.07) at the four sites, the n-alkanal homologues with carbon number
405 from C_8 to C_{20} mainly originate from anthropogenic emissions or OH oxidation of anthropogenic
406 fossil-derived hydrocarbons. The particle-bound n-alkanals exhibited a similar distribution of carbon
407 number from January to April at four sites, and they had the same C_{\max} at C_8 with concentration 28.6
408 ng m^{-3} at RU, 50.3 ng m^{-3} at WM, 53.0 ng m^{-3} at EL and 141 ng m^{-3} at MR, respectively. This
409 compound may be a fragmentation product, oxidation product or primary emission. In addition, the
410 distribution of n-alkanals had a second concentration peak at C_{15} (MR) and C_{18} (RU, WM, and EL).
411 The C_{18} compound was observed accounting for the highest percentage of the total mass of n-
412 alkanals in some rural aerosol samples (Gogou et al., 1996) in Crete. Andreou and Rapsomanikis
413 reported the C_{\max} as C_{15} or C_{17} in Athens (Andreou and Rapsomanikis, 2009) and attributed this to
414 the oxidation of n-alkanes. However, a C_{\max} at C_{26} or C_{28} in urban Crete (Gogou et al., 1996) was
415 observed, suggestive of biogenic input. The homologue distribution and CPI of n-alkanals in this
416 study differed from those previous reports, and demonstrated weak biogenic input and a strong

417 impact of anthropogenic activities in the London samples.

418

419 In this study, n-alkan-2-ones have similar homologue distributions and C_{\max} (C_{19} or C_{20}) (Table 2)
420 at RU, WM and EL sites, and the total concentration from C_{16} to C_{23} accounts for 76.0%, 76.1% and
421 68.0% of \sum n-alkan-2-ones, respectively. The CPI values for n-alkan-2-ones ranged from 0.57 to
422 1.23 at the RU, MR and WM sites and were not indicative of major biogenic input, and were
423 considered to mainly originate from anthropogenic activities and OH oxidation of anthropogenic n-
424 alkanes. It is however notable that the CPI values for both the 2-ketones and 3-ketones exceed
425 those for the alkanals (see Table 1), suggesting a contribution from contemporary biogenic sources,
426 possibly wood smoke and cooking. At EL, the CPI of 1.57 is ~~probably~~clearly indicative of a
427 biogenic contribution in suburban south London. A difference was observed at the MR site, the n-
428 alkan-2-ones with carbon atoms numbering from C_{12} to C_{18} accounting for 72.0% of \sum n-alkan-2-
429 ones, with the C_{\max} being at C_{16} . These data suggest a contribution of primary emissions from
430 traffic at MR, but a dominant background, probably substantially secondary, at the other sites. The
431 C_{\max} of n-alkan-3-ones was at C_{16} at the MR site, at EL, $C_{\max} = C_{16}$, WM, $C_{\max} = C_{17}$ and at RU, C_{\max}
432 = C_{17} , respectively.

433

434 **3.32.2 The ratios of n-alkanes/n-alkanals**

435 Diesel engine emission studies have been conducted previously in our group; details of the engine set
436 up and exhaust sampling system are given elsewhere (Alam et al., 2016b). Briefly, the steady-state
437 diesel engine operating conditions were at a load of 5.90 bar mean effective pressure (BMEP) and a

438 speed of 1800 revolutions per minute (RPM), and samples (n=14) were collected both before a diesel
439 oxidation catalyst (DOC) and after a diesel particulate filter (DPF). The n-alkanes (C₁₂ - C₃₇) and 1-
440 alkanals (C₉ - C₁₈) were quantified in the particle samples, while n-alkanones were not identified
441 because their concentrations were lower than the limits of (detection 0.01–0.15 ng m⁻³). The emission
442 concentrations of n-alkanals ranged from 7.10 to 53.2 µg m⁻³ (before DOC) and 1.20 to 11.5 µg m⁻³
443 (after DPF), respectively, and the ratios of alkanes/alkanals (~~C₁₂C₁₃~~-C₁₈) with the same carbon atom
444 numbers ranged from 0.15 to 0.23 (before DOC) and 0.52 to 7.60 (after DPF). The n-alkane/n-alkanal
445 (~~C₁₂C₁₃~~-C₁₈) ratio at MR ranged from 0.92–30 to 5.703, while average ratios of 27.614.9 (RU),
446 22.411.5 (WM) and 15.414.7 (EL) were obtained, respectively. The similarity of the n-alkanes/n-
447 alkanal ratio between MR and the engine studies (after DPF) strongly suggests that diesel vehicle
448 emissions were the main source of 1-alkanals at MR. The higher ratios at the other sites may be due
449 to greater airmass aging and loss of alkanals due to their higher reactivity (Chacon-Madrid and
450 Donahue, 2011; Chacon-Madrid et al., 2010).

451
452 The emission factors of total alkanes from diesel engines are reported to be 7 times greater than
453 gasoline engines (Perrone et al., 2014), with n-alkanals with carbon atoms numbering lower than C₁₁
454 being quantified in the exhaust from gasoline engines (Schauer et al., 2002b; Gentner et al., 2013).
455 The n-alkane/n-alkanal (C₈-C₁₀) ratio with the same carbon numbers ranged from 5.60 to 14.3
456 (Schauer et al., 2002b), suggesting that gasoline combustion may be another potential source of
457 atmospheric n-alkanals.

458

459 ~~Studies of n-alkanals showed that aldehydes have high reactivity when the OH radical attacks the~~
460 ~~aldehyde moiety (Chacon Madrid and Donahue, 2011; Chacon Madrid et al., 2010), and the rate~~
461 ~~constants are more than 3 times those of n-alkanes with the same carbon number. The mechanism~~
462 ~~and rate constants of H-abstraction by OH detailed in the Master Chemical Mechanism (MCM,~~
463 ~~v3.3.1), were obtained via <http://mem.leeds.ac.uk/MCM>, and used in the evaluation of our data.~~

464

465 **3.32.3 Correlation analysis**

466 Insights into the sources of carbonyls can be gained from intra-site ~~from~~ correlation analysis with
467 black carbon (BC) and NO_x. This ~~has the advantage of comparing relative concentrations of~~
468 ~~pollutants, rather than absolute concentrations. The latter is more informative than comparisons~~
469 ~~between sites when sampling did not take place simultaneously, as concentrations~~ are strongly
470 affected by weather conditions, making inter-site comparisons difficult ~~to interpret when sampling~~
471 ~~did not occur simultaneously~~. In London, both black carbon and NO_x arise very substantially from
472 diesel vehicle emissions (Liu et al., 2014; Harrison et al., 2012; Harrison and Beddows, 2017), and
473 hence these are good measures of road traffic activity. The concentrations of BC were
474 simultaneously determined by the online instruments during the sampling periods, with the average
475 concentrations of 1.34, 1.94 and 3.58 µg m⁻³ at the RU, WM and MR sites, respectively. The data
476 for NO_x were provided by the national network sites, with the average concentrations of 23.4 and
477 202 µg m⁻³ at the EL and MR sites, respectively. At the MR site, the concentrations of BC and NO_x
478 averaged 5.00 µg m⁻³ and 281 µg m⁻³ when southerly winds were dominant compared to 2.60 and
479 128 µg m⁻³ for northerly winds. All correlations were carried out with the sum of particle and vapour
480 phases for the carbonyl compounds, and strong ($r^2 = 0.87$) and weak ($r^2 = 0.12$) correlations between

481 BC and NO_x were obtained when the southerly and northerly winds were prevalent at MR,
482 respectively. Marylebone Road is a street canyon site where a vortex circulation is established by
483 the wind. The effect is that on northerly wind sectors the sampling site on the southern side of the
484 road samples near-background air, while on southerly wind sectors, the traffic pollution is carried
485 to the sampling site, leading to elevated pollution levels affected heavily by the traffic emissions.
486 The strong correlation between BC and NO_x with southerly wind sectors is a reflection of their
487 emission from road traffic. In addition, the correlations between n-alkanals (C₈-C₂₀) and BC, and
488 between n-alkanals (C₈-C₂₀) and NO_x were calculated to assess the contribution of vehicular
489 emissions (Table S3). The results showed that the correlations (r^2) between n-alkanals and BC
490 gradually decreased from 0.61 (C₉) to 0.34 (C₂₀) at MR when the southerly winds were prevalent,
491 indicating that the distribution of n-alkanals, and especially the lower MW compounds, was
492 significantly impacted by the vehicular exhaust emissions. The average correlations at MR
493 (southerly winds) between n-alkanals and BC, and between n-alkanals and NO_x were $r^2 = 0.47$ and
494 $r^2 = 0.32$, respectively. These moderate correlations demonstrated that the vehicular emissions were
495 a ~~substantial~~ source of n-alkanals at MR, and ~~result in~~ contribute to the high background
496 concentrations of n-alkanals in London. The other probable sources of n-alkanals include cooking
497 emissions, wood burning, photooxidation of hydrocarbons and industrial emissions. Poorer
498 correlations between n-alkanals and BC (average $r^2 = 0.15$), and between n-alkanals and NO_x
499 (average $r^2 = 0.15$) were observed at MR in the north London background air sampled when
500 northerly winds were prevalent. There were very weak correlations (average $r^2 < 0.10$) between n-
501 alkanals and BC, and between n-alkanals and NO_x at the RU, WM and EL sites, which may be
502 attributable to the high chemical reactivity of n-alkanals. High concentrations of furanones (γ -

503 lactones) are generated via the photo-oxidation reaction of n-alkanals (Alves et al., 2001), and the
504 total concentrations (particle and gas) were up to 376, 279, 347 and 318 ng m⁻³ at RU, WM, WL,
505 and MR, respectively for the sum of furanone homologues (from 5-propyldihydro-2(3H)-furanone
506 to 5-tetradecyldihydro-2(3H)-furanone).

507

508 The relationships (r^2 values) between BC and NO_x and the n-alkan-2-ones were low at all sites, but
509 notably higher with southerly winds at MR (average $r^2 = 0.33$ and 0.35 for BC and NO_x respectively)
510 than for northerly winds ($r^2 = 0.16$ and 0.03 respectively). This is strongly suggestive of a
511 contribution from vehicle exhaust to n-alkan-2-one concentrations, but smaller than that for n-
512 alkanals. In the case of the n-alkan-3-ones, correlations averaged $r^2 = 0.25$ with BC and $r^2 = 0.21$ for
513 NO_x in southerly winds, compared to $r^2 = 0.08$ and $r^2 = 0.05$ respectively for northerly winds. This
514 is also suggestive of a small, but not negligible contribution of vehicle emissions to n-alkan-3-ones.
515 The very low correlations observed in background air for both n-alkan-2-ones and n-alkan-3-ones
516 with BC and NO_x are suggestive of the importance of non-traffic sources, probably including
517 oxidation of n-alkanes. Both compound groups were below detection limit in the analyses of diesel
518 exhaust. The considerable predominance ~~for-of~~ n-alkan-2-one over n-alkan-3-one concentrations
519 may be indicative of a formation pathway from oxidation of condensed phase n-alkanes, but this is
520 speculative as primary emissions may be dominant.

521

522 **3.4.3 The Partition Between Particle and Gas Phase Gas and Particle Phase Partitioning**

523 The partitioning coefficient K_p between particles and vapour was calculated in this study according
524 to the following equation defined by Pankow (1994):

525

$$526 \quad K_p = \frac{C_p}{C_g * TSP}$$

527

528 Where, C_p and C_g ($\mu\text{g m}^{-3}$) are the concentration of the compounds in the particulate phase and
529 gaseous phase, respectively. TSP is the concentration of total suspended particulate matter ($\mu\text{g m}^{-3}$),
530 which was estimated from the PM_{10} concentration ($\text{PM}_{10}/\text{TSP} = 0.80$), and daily average PM_{10}
531 concentrations were taken from the national network sites (see Table S5). The partitioning
532 coefficients K_p calculated from our data and the percentages in the particulate form are presented in
533 Table 2. For the three types of carbonyls, the n-alkanals $>C_{16}$, n-alkan-2-ones $>C_{19}$, and n-alkan-3-
534 ones $>C_{18}$ ~~were assumed to have negligible~~ the vapour concentrations were below detection limit,
535 and the partitioning into the particulate phase gradually increased from C_8 to high molecular weight
536 compounds.

537

538 Log K_p was regressed against vapour pressure (VP_T) for the relevant temperature derived from
539 UManSysProp (<http://umansysprop.seaes.manchester.ac.uk/>) according to the following equation:

540

$$541 \quad \text{Log } K_p = m \log(\text{VP}_T) + b$$

542

543 The calculated log K_p versus log (VP_T) for the three types of carbonyls was calculated for each day,
544 and the results appear in the Table S4. Data from four sites were over the temperature range 0.40–
545 15.3 °C. A good fit to the data for n-alkan-2-ones ($r^2 = 0.54$ – 0.94 at RU, 0.64 – 0.93 at WM, 0.43 –

546 0.95 EL and 0.45-0.89 at MR) was obtained. It is notable that the fit to the regression equation as
547 indicated by the r^2 value is appreciably higher at the MR site than at the other sites, especially in the
548 case of the alkan-3-ones. This is not easily explained, except perhaps by an increased particle surface
549 area at the MR site which may enhance the kinetics of gas-particle exchange, leading to partitioning
550 which is closer to equilibrium.

551

552 4. CONCLUSIONS

553 Three groups of carbonyl compounds were determined in the particle and gaseous phase in London
554 and concentrations are reported for n-alkanals (C_8 - C_{20}), n-alkan-2-ones (C_8 - C_{26}) and n-alkan-3-ones
555 (C_8 - C_{19}). The Marylebone Road site has the highest concentration of particle-bound n-alkanals, and
556 the average total concentration was up to 682 ng m^{-3} , followed by 167 ng m^{-3} at EL, 117 ng m^{-3} at
557 WM and 82.6 ng m^{-3} at RU. The particulate n-alkanals were abundant in all samples at all four
558 measurement sites, accounting for more than 56.3% of total particle carbonyls. In addition, the
559 average total particle concentrations of n-alkan-2-ones and n-alkan-3-ones at four measurement sites
560 were in the range of 58.5 - 186 ng m^{-3} and 5.65 - 39.4 ng m^{-3} , respectively. Diagnostic criteria,
561 including molecular distribution, CPI, C_{max} , ratios and correlations, were used to assess the sources
562 and their contributions to carbonyl compounds. The three groups of carbonyls have similar
563 molecular distributions and C_{max} values at the four measurement sites, and their low CPI values
564 (0.41-1.57) at the four sites indicate a weak biogenic input during sampling campaigns. Heavily
565 traffic-influenced air and urban background air were measured at the MR site when southerly and
566 northerly winds were prevalent respectively; correlations of $r^2 = 0.47$ and $r^2=0.32$ were obtained
567 between n-alkanals and BC, and between between n-alkanals and NO_x , respectively in southerly

568 winds. Vehicle emissions appear to be an important source of n-alkanals, which is confirmed by the
569 similar ratios of n-alkanes/n-alkanals measured at MR (~~0.30-5.75~~~~0.92-5.03~~) and in diesel engine
570 exhaust studies (0.52-7.6), resulting in a high background concentration in London. In addition, the
571 OH-initiated heterogeneous reactions of n-alkanes appear to be important sources of n-alkanones,
572 even though weak contributions from vehicular exhaust emissions were suggested by correlation
573 analysis with BC and NO_x in southerly winds at MR. Anthropogenic primary sources such as
574 cooking (Abdullahi et al., 2013) appear to may account for a ~~large~~ proportion of the alkan-2-one and
575 alkan-3-one concentrations measured in London, in addition to the secondary contribution from
576 alkane oxidation. Any contribution from cooking or wood combustion is likely to be small, or the
577 CPI would be greater.

578

579 In addition, the partitioning coefficients of carbonyls were determined from the relative proportions
580 of the particle and gaseous phases of individual compounds. The results of field measurements of
581 partitioning between particle and vapour phases showed generally a better fit at MR than at the other
582 three sites. The n-alkan-2-ones have a better fit at four sites than the n-alkanals and n-alkan-3-ones,
583 with $r^2 = 0.78-72$ (~~0.5449-0.9457~~) at RU, $0.85-76$ (~~0.6455-0.9387~~) at WM, 0.74 (0.43-0.95) EL and
584 0.70 (0.45-0.89) at MR, respectively in a regression of log K_p versus the compound vapour pressure.
585 This most likely reflects the slow formation of the alkan-2-ones as secondary constituents, closer to
586 phase equilibrium than the largely emitted alkanals which would be spatially far more variable.
587 The higher r^2 values for the alkan-2-ones than alkan-3-ones may reflect the higher concentrations,
588 and hence better analytical precision for the former compound group.

589

590 **ACKNOWLEDGEMENTS**

591 Primary collection of samples took place during the FASTER project which was funded by the
592 European Research Council (ERC-2012-AdG, Proposal No. 320821). The authors would also like
593 to thank the China Scholarship Council (CSC) for support to R.L., and the Natural Environment
594 Research Council for support under the Air Pollution and Human Health (APHH) programme
595 (NE/N007190/1).

596 **REFERENCE**

597

598 Abdullahi, K.L., Delgado-Saborit, J.M., and R.M. Harrison: Emissions and indoor concentrations
599 of particulate matter and its specific chemical components from cooking: A review, Atmos.
600 Environ., 71, 260-294, <http://dx.doi.org/10.1016/j.atmosenv.2013.01.061>, 2013.
601

602 Alam, M. S., Stark, C., and Harrison, R. M.: Using variable ionization energy time-of-flight mass
603 spectrometry with comprehensive GC×GC to identify isomeric species, *Anal. Chem.*, 88, 4211-
604 4220, <http://www.doi.org/10.1021/acs.analchem.5b03122>, 2016a.

605

606 Alam, M. S., Zeraati-Rezaei, S., Stark, C. P., Liang, Z., Xu, H., and Harrison, R. M.: The
607 characterisation of diesel exhaust particles - composition, size distribution and partitioning,
608 *Faraday. Discuss.*, 189, 69-84, <http://www.doi.org/10.1039/C5FD00185D>, 2016b.

609

610 Alam, M. S., Zeraati-Rezaei, S., Liang, Z., Stark, C., Xu, H., MacKenzie, A. R., and Harrison, R.
611 M.: Mapping and quantifying isomer sets of hydrocarbons ($\geq C_{12}$) in diesel exhaust, lubricating oil
612 and diesel fuel samples using GC×GC-ToF-MS, *Atmos. Meas. Tech.*, 11, 3047,
613 <https://doi.org/10.5194/amt-11-3047-2018>, 2018.

614

615 Algrim, L. B., and Ziemann, P. J.: Effect of the Keto Group on yields and composition of organic
616 aerosol formed from OH radical-initiated reactions of ketones in the presence of NO_x, *J. Phys.*
617 *Chem. A.*, 120, 6978-6989, <http://www.doi.org/10.1021/acs.jpca.6b05839>, 2016.

618

619 Alves, C., Pio, C., and Duarte, A.: Composition of extractable organic matter of air particles from
620 rural and urban Portuguese areas, *Atmos. Environ.*, 35, 5485-5496, [https://doi.org/10.1016/S1352-](https://doi.org/10.1016/S1352-2310(01)00243-6)
621 [2310\(01\)00243-6](https://doi.org/10.1016/S1352-2310(01)00243-6), 2001.

622

623 Andreou, G., and Rapsomanikis, S.: Origins of n-alkanes, carbonyl compounds and molecular
624 biomarkers in atmospheric fine and coarse particles of Athens, Greece, *Sci. Total. Environ.*, 407,
625 5750-5760, <http://dx.doi.org/10.1016/j.scitotenv.2009.07.019>, 2009.

626

627 Aschmann, S. M., Arey, J., and Atkinson, R.: Atmospheric chemistry of three C₁₀ alkanes, *J. Phys.*
628 *Chem. A.*, 105, 7598-7606, <http://www.doi.org/10.1021/jp010909j>, 2001.

629

630 Bray, E., and Evans, E.: Distribution of n-paraffins as a clue to recognition of source beds,
631 *Geochim. Cosmochim. Ac.*, 22, 2-15, [https://doi.org/10.1016/0016-7037\(61\)90069-2](https://doi.org/10.1016/0016-7037(61)90069-2), 1961.

632

633 Chacon-Madrid, H., and Donahue, N.: Fragmentation vs. functionalization: chemical aging and
634 organic aerosol formation, *Atmos. Chem. Phys.*, 11, 10553-10563, [https://doi.org/10.5194/acp-11-](https://doi.org/10.5194/acp-11-10553-2011)
635 [10553-2011](https://doi.org/10.5194/acp-11-10553-2011), 2011.

636

637 Chacon-Madrid, H. J., Presto, A. A., and Donahue, N. M.: Functionalization vs. fragmentation: n-
638 aldehyde oxidation mechanisms and secondary organic aerosol formation, *Phys. Chem. Chem.*
639 *Phys.*, 12, 13975-13982, <http://www.doi.org/10.1039/C0CP00200C>, 2010.

640 Cheng, Y., Li, S.-M., Leithead, A., and Brook, J. R.: Spatial and diurnal distributions of n-alkanes
641 and n-alkan-2-ones on PM 2.5 aerosols in the Lower Fraser Valley, Canada, *Atmos. Environ.*, 40,
642 2706-2720, <https://doi.org/10.1016/j.atmosenv.2005.11.066>, 2006.

643

644 Duan, H., Liu, X., Yan, M., Wu, Y., and Liu, Z.: Characteristics of carbonyls and volatile organic
645 compounds (VOCs) in residences in Beijing, China, *Front. Env. Sci. Eng.*, 10, 73-84,
646 <http://www.doi.org/10.1007/s11783-014-0743-0>, 2016.

647

648 Gentner, D. R., Worton, D. R., Isaacman, G., Davis, L. C., Dallmann, T. R., Wood, E. C., Herndon,
649 S. C., Goldstein, A. H., and Harley, R. A.: Chemical composition of gas-phase organic carbon
650 emissions from motor vehicles and implications for ozone production, *Environ. Sci. Technol.*, 47,
651 11837-11848, <http://www.doi.org/10.1021/es401470e>, 2013.

652

653 Gogou, A., Stratigakis, N., Kanakidou, M., and Stephanou, E. G.: Organic aerosols in Eastern
654 Mediterranean: components source reconciliation by using molecular markers and atmospheric back
655 trajectories, *Org. Geochem.*, 25, 79-96, [https://doi.org/10.1016/S0146-6380\(96\)00105-2](https://doi.org/10.1016/S0146-6380(96)00105-2), 1996.

656

657 Han, Y., Kawamura, K., Chen, Q., and Mochida, M.: Formation of high-molecular-weight
658 compounds via the heterogeneous reactions of gaseous C8–C10 n-aldehydes in the presence of
659 atmospheric aerosol components, *Atmos. Environ.*, 126, 290-297,
660 <http://dx.doi.org/10.1016/j.atmosenv.2015.11.050>, 2016.

661

662 Harrison, R., Dall'Osto, M., Beddows, D., Thorpe, A., Bloss, W., Allan, J., Coe, H., Dorsey, J.,
663 Gallagher, M., and Martin, C.: Atmospheric chemistry and physics in the atmosphere of a
664 developed megacity (London): an overview of the REPARTEE experiment and its conclusions,
665 *Atmos. Chem. Phys.*, 12, 3065-3114, <https://doi.org/10.5194/acp-12-3065-2012>, 2012.

666

667 Harrison, R. M., and Beddows, D. C.: Efficacy of recent emissions controls on road vehicles in
668 Europe and implications for public health, *Sci. Rep-UK.*, 7, 1152,
669 <http://www.doi.org/10.1038/s41598-017-01135-2>, 2017.

670

671 Kwok, E. S., and Atkinson, R.: Estimation of hydroxyl radical reaction rate constants for gas-phase
672 organic compounds using a structure-reactivity relationship: an update, *Atmos. Environ.*, 29, 1685-
673 1695, [https://doi.org/10.1016/1352-2310\(95\)00069-B](https://doi.org/10.1016/1352-2310(95)00069-B), 1995.

674

675 [Lim, Y. B., and Ziemann, P.J.: Chemistry of secondary organic aerosol formation from OH](https://doi.org/10.1080/02786820902802567)
676 [radical-initiated reactions of linear, branched, and cyclic alkanes in the presence of NO_x, *Aerosol*](https://doi.org/10.1080/02786820902802567)
677 [Sci. Technol.](https://doi.org/10.1080/02786820902802567), 43, 604-619, <https://doi.org/10.1080/02786820902802567>, 2009.

678

679 Liu, D., Allan, J., Young, D., Coe, H., Beddows, D., Fleming, Z., Flynn, M., Gallagher, M.,
680 Harrison, R., and Lee, J.: Size distribution, mixing state and source apportionments of black carbon
681 aerosols in London during winter time, *Atmos. Chem. Phys.*, 14, [https://doi.org/10.5194/acp-14-](https://doi.org/10.5194/acp-14-10061-2014)
682 10061-2014, 2014.

683

684 Oliveira, T. S., Pio, C., Alves, C. A., Silvestre, A. J., Evtuygina, M., Afonso, J., Fialho, P., Legrand,
685 M., Puxbaum, H., and Gelencsér, A.: Seasonal variation of particulate lipophilic organic
686 compounds at nonurban sites in Europe, *J. Geophys. Res-Atmos.*, 112,
687 <https://doi.org/10.1029/2007JD008504> 2007.
688

689 Oros, D. R., and Simoneit, B. R. T.: Identification and emission rates of molecular tracers in coal
690 smoke particulate matter, *Fuel.*, 79, 515-536, [http://dx.doi.org/10.1016/S0016-2361\(99\)00153-2](http://dx.doi.org/10.1016/S0016-2361(99)00153-2),
691 2000.
692

693 Pankow, J. F.: An absorption model of gas/particle partitioning of organic compounds in the
694 atmosphere, *Atmos. Environ.*, 28, 185-188, [https://doi.org/10.1016/1352-2310\(94\)90093-0](https://doi.org/10.1016/1352-2310(94)90093-0), 1994.
695

696 Perrone, M. G., Carbone, C., Faedo, D., Ferrero, L., Maggioni, A., Sangiorgi, G., and Bolzacchini,
697 E.: Exhaust emissions of polycyclic aromatic hydrocarbons, n-alkanes and phenols from vehicles
698 coming within different European classes, *Atmos. Environ.*, 82, 391-400,
699 <https://doi.org/10.1016/j.atmosenv.2013.10.040>, 2014.
700

701 Rogge, W. F., Hildemann, L. M., Mazurek, M. A., and Cass, G. R.: Sources of fine organic aerosol.
702 9. Pine, oak, and synthetic log combustion in residential fireplaces, *Environ. Sci. Technol.*, 32, 13-
703 22, <http://www.doi.org/10.1021/es960930b>, 1998.
704

705 Ruehl, C. R., Nah, T., Isaacman, G., Worton, D. R., Chan, A. W. H., Kolesar, K. R., Cappa, C. D.,
706 Goldstein, A. H., and Wilson, K. R.: The influence of molecular structure and aerosol phase on the
707 heterogeneous oxidation of normal and branched alkanes by OH, *J. Phys. Chem. A.*, 117, 3990-
708 4000, <http://www.doi.org/10.1021/jp401888q>, 2013.
709

710 [Schauer, J. J., Kleeman M. J., Cass, G. R., and Simoneit, B. R. T.: Measurement of emissions](#)
711 [from air pollution sources. 2. C1 through C30 organic compounds from medium duty diesel trucks,](#)
712 [Environ. Sci.Technol., 33, 1578-1587, 10.1021/es980081n, 1999a.](#)
713

714 Schauer, J. J., Kleeman, M. J., Cass, G. R., and Simoneit, B. R. T.: Measurement of emissions from
715 air pollution sources. 1. C1 through C29 organic compounds from meat charbroiling, *Environ. Sci.*
716 *Technol.*, 33, 1566-1577, <http://www.doi.org/10.1021/es980076j>, 1999**b**.
717

718 Schauer, J. J., Kleeman, M. J., Cass, G. R., and Simoneit, B. R. T.: Measurement of emissions from
719 air pollution sources. 3. C1–C29 organic compounds from fireplace combustion of wood, *Environ.*
720 *Sci. technol.*, 35, 1716-1728, <http://www.doi.org/10.1021/es001331e>, 2001.
721

722 Schauer, J. J., Kleeman, M. J., Cass, G. R., and Simoneit, B. R. T.: Measurement of emissions from
723 air pollution sources. 4. C1–C27 organic compounds from cooking with seed oils, *Environ. Sci.*
724 *Technol.*, 36, 567-575, <http://www.doi.org/10.1021/es002053m>, 2002a.
725

726 Schauer, J. J., Kleeman, M. J., Cass, G. R., and Simoneit, B. R. T.: Measurement of emissions from
727 air pollution sources. 5. C1–C32 organic compounds from gasoline-powered motor vehicles,
728 *Environ. Sci. Technol.*, 36, 1169-1180, <http://www.doi.org/10.1021/es0108077>, 2002b.

729
730
731
732
733
734
735
736
737
738
739
740
741
742
743
744
745
746
747
748
749
750
751
752
753
754
755
756
757
758
759
760
761
762
763

Schilling Fahnestock, K. A., Yee, L. D., Loza, C. L., Coggon, M. M., Schwantes, R., Zhang, X., Dalleska, N. F., and Seinfeld, J. H.: Secondary organic aerosol composition from C12 alkanes, *J. Phys. Chem. A.*, 119, 4281-4297, <http://www.doi.org/10.1021/jp501779w>, 2015.

[Simoneit, B. R. T., Cox, R. E., and Standley, L. J.: Organic matter of the troposphere - IV. Lipids in harmattan aerosols of Nigeria, *Atmos. Environ.*, 22, 983-1004, \[https://doi.org/10.1016/0004-6981\\(88\\)90276-4\]\(https://doi.org/10.1016/0004-6981\(88\)90276-4\), 1967.](#)

[UK-Air, <https://uk-air.defra.gov.uk>, last accessed 16 December 2018.](https://uk-air.defra.gov.uk)

Yee, L. D., Craven, J. S., Loza, C. L., Schilling, K. A., Ng, N. L., Canagaratna, M. R., Ziemann, P. J., Flagan, R. C., and Seinfeld, J. H.: Secondary organic aerosol formation from low-NO_x photooxidation of dodecane: Evolution of multigeneration gas-phase chemistry and aerosol composition, *J. Phys. Chem. A.*, 116, 6211-6230, <http://www.doi.org/10.1021/jp211531h>, 2012.

Zhang, H., Worton, D. R., Shen, S., Nah, T., Isaacman-VanWertz, G., Wilson, K. R., and Goldstein, A. H.: Fundamental time scales governing organic aerosol multiphase partitioning and oxidative aging, *Environ. Sci. Technol.*, 49, 9768-9777, <http://www.doi.org/10.1021/acs.est.5b02115>, 2015.

Zhao, Y., Hu, M., Slanina, S., and Zhang, Y.: The molecular distribution of fine particulate organic matter emitted from Western-style fast food cooking, *Atmos. Environ.*, 41, 8163-8171, <http://dx.doi.org/10.1016/j.atmosenv.2007.06.029>, 2007a.

Zhao, Y., Hu, M., Slanina, S., and Zhang, Y.: Chemical compositions of fine particulate organic matter emitted from Chinese cooking, *Environ. Sci. Technol.*, 41, 99-105, <http://www.doi.org/10.1021/es0614518>, 2007b.

[Ziemann, P. J.: Effects of molecular structure on the chemistry of aerosols formation from the OH-radical-initiated oxidation of alkanes and alkenes, *Intl. Rev. Phys. Chem.*, 30, 161-195, <https://doi.org/10.1080/0144235X.2010.550728>, 2011.](#)

764 **TABLE LEGENDS**

765

766 Table 1. The carbon preference index (CPI) and C_{max} for n-alkanals, n-alkan-2-ones, and
767 n-alkan-3-ones in this study and published data.

768

769 Table 2. Percentages of particle phase form and the partitioning coefficient K_p .

770

771 **FIGURE LEGENDS**

772

773 Figure 1. Map of the sampling sites. RU-Regents University (15 m above ground); WM-
774 University of Westminster (20 m above ground); EL-Eltham; MR-Marylebone Road
775 (south side).

776

777 Figure 2. The average total concentration of particle-bound n-alkanals (C_8-C_{20}), n-alkan-2-ones
778 (C_8-C_{26}), and n-alkan-3-ones (C_8-C_{19}), for each sampling period and site. The error bars
779 indicate one standard deviation.

780

781 Figure 3. Time series of particle-bound Σn -alkanals, Σn -alkan-2-ones and Σn -alkan-3-ones at
782 RU, WM, EL, and MR sites.

783

784 Figure 4. The molecular distribution of particle-bound carbonyl compounds at four sites (RU,
785 WM, EL, and MR).

786

787

788

Table 1. The carbon preference index (CPI) and C_{max} for n-alkanals, n-alkan-2-ones, and n-alkan-3-ones in this study and published data.

Location Sampling site	Sampling period	n-alkanals		n-alkan-2-ones		n-alkan-3-ones		Reference
		CPI	C_{max}	CPI	C_{max}	CPI	C_{max}	
RU, surrounded by Regent's Park, 15 m above ground	23 Jan - 19 Feb	0.52	C ₈	1.23	C ₁₉	1.30	C ₁₇	Present study
WM, 20 m above ground	24 Jan - 20 Feb	0.41	C ₈	0.99	C ₂₀	1.26	C ₁₇	Present study
EL, suburb of London	23 Feb - 21 Mar	0.71	C ₈	1.57	C ₂₀	1.04	C ₁₆	Present study
MR, adjacent to Marylebone road	22 Mar - 18 Apr	1.07	C ₈	0.57	C ₁₆	1.12	C ₁₆	Present study
Athens, Athinas St. Urban roadside	August March	1.49	C ₁₅ , C ₁₇	1.09 3.26	C ₁₈ , C ₂₁ , C ₁₉ C ₂₁ , C ₁₉ , C ₂₀			(Andreou and Rapsomanikis, 2009)
Athens, AEDA, Urban, 20 m above ground	March			2.41	C ₁₉ , C ₁₈ , C ₂₀			(Andreou and Rapsomanikis, 2009)
Heraklion, Greece Urban 15 m above ground	Spring /summer	0.80–1.40	C ₂₆ , C ₂₈	1.30–1.80	C ₂₃ , C ₂₉ , C ₃₁			(Gogou et al., 1996)
Vancouver, Canada Roadway tunnel				1.33	C ₁₇ , C ₁₉			(Cheng et al., 2006)
Aveiro, Portugal Suburban	Summer Winter		C ₂₂ , C ₂₃ , C ₂₆		C ₂₆ , C ₂₈ , C ₃₀			(Oliveira et al., 2007)
K-Puszta, Hungary	Summer		C ₂₄ , C ₂₆ , C ₂₈		C ₂₄ , C ₂₆ , C ₂₈			

Table 2. Percentages of particle phase form and the partitioning coefficient K_p ($m^3 \mu g^{-1}$).

	RU						WM					
	n-alkanals		n-alkan-2-ones		n-alkan-3-ones		n-alkanals		n-alkan-2-ones		n-alkan-3-ones	
	%	K_p	%	K_p	%	K_p	%	K_p	%	K_p	%	K_p
C ₈	82.9	1.16E-04	18.4	5.37E-06	23.9	7.47E-06	80.2	9.09E-05	13.3	3.43E-06	34.1	1.16E-05
C ₉	69.2	5.37E-05	14.5	4.03E-06	16.6	4.74E-06	60.5	3.43E-05	15.6	4.16E-06	28.7	9.05E-06
C ₁₀	75.3	7.27E-05	13.6	3.77E-06	7.43	1.92E-06	82.1	1.03E-04	14.4	3.77E-06	23.3	6.82E-06
C ₁₁	45.5	1.99E-05	21.4	6.49E-06	12.8	3.49E-06	62.4	3.72E-05	20.1	5.65E-06	36.3	1.28E-05
C ₁₂	74.8	7.08E-05	25.0	7.96E-06	31.3	1.09E-05	73.7	6.29E-05	28.8	9.07E-06	22.7	6.60E-06
C ₁₃	82.9	1.15E-04	61.0	3.74E-05	35.4	1.31E-05	82.2	1.04E-04	48.9	2.14E-05	62.5	3.74E-05
C ₁₄	82.8	1.15E-04	49.5	2.34E-05	35.5	1.31E-05	75.8	7.04E-05	31.8	1.05E-05	25.6	7.74E-06
C ₁₅	99.5	5.01E-03	84.1	1.26E-04	50.5	2.44E-05	*100		85.0	1.27E-04	68.5	4.87E-05
C ₁₆	100*		91.4	2.53E-04	70.3	5.64E-05	*100		89.6	1.93E-04	91.7	2.47E-04
C ₁₇	100*		91.5	2.55E-04	*100		*100		85.9	1.36E-04	91.5	2.42E-04
C ₁₈	100*		94.1	3.80E-04	*100		*100		84.8	1.26E-04	99.4	4.02E-03
C ₁₉	100*		99.1	2.69E-03			*100		*100			
C ₂₀	100*		100*				*100		*100			
C ₂₁			100*						*100			
C ₂₂			100*						*100			
C ₂₃			100*						*100			
C ₂₄			100*						*100			
C ₂₅			100*						*100			
C ₂₆			100*						*100			

	EI						MR					
	n-alkanals		n-alkan-2-ones		n-alkan-3-ones		n-alkanals		n-alkan-2-ones		n-alkan-3-ones	
	%	K _p	%	K _p	%	K _p	%	K _p	%	K _p	%	K _p
C ₈	92.7	6.53E-04	24.9	1.72E-05	31.9	2.43E-05	90.0	2.94E-04	28.2	1.28E-05	43.0	2.46E-05
C ₉	92.2	6.16E-04	38.0	3.18E-05	44.4	4.15E-05	89.9	2.89E-04	27.0	1.20E-05	39.1	2.09E-05
C ₁₀	90.5	4.96E-04	47.6	4.70E-05	47.0	4.59E-05	91.7	3.62E-04	61.1	5.12E-05	20.4	8.33E-06
C ₁₁	87.0	3.47E-04	72.3	1.35E-04	81.9	2.34E-04	87.4	2.26E-04	50.2	3.28E-05	33.1	1.61E-05
C ₁₂	92.9	6.73E-04	83.4	2.60E-04	66.4	1.02E-04	93.0	4.30E-04	88.5	2.51E-04	28.1	1.28E-05
C ₁₃	95.6	1.12E-03	82.2	2.40E-04	65.7	9.92E-05	96.1	8.04E-04	87.7	2.33E-04	46.2	2.79E-05
C ₁₄	91.4	5.52E-04	90.3	4.80E-04	59.1	7.48E-05	95.2	6.51E-04	95.9	7.61E-04	72.0	8.38E-05
C ₁₅	96.7	1.53E-03	94.5	8.98E-04	84.4	2.80E-04	*100		96.9	1.02E-03	83.8	1.69E-04
C ₁₆	*100		96.7	1.41E-03	89.0	4.18E-04	*100		96.4	8.70E-04	88.0	2.38E-04
C ₁₇	*100		95.1	1.00E-03	81.5	2.28E-04	*100		96.0	7.73E-04	88.0	2.39E-04
C ₁₈	*100		64.6	9.44E-05	85.0	2.93E-04	*100		92.5	4.04E-04	*100	
C ₁₉	*100		*100				*100		*100		*100	
C ₂₀	*100		*100				*100		*100		*100	
C ₂₁			*100						*100		*100	
C ₂₂			*100						*100		*100	
C ₂₃			*100						*100		*100	
C ₂₄									*100		*100	

* For compounds marked with an asterisk, the particulate phase was quantified, but the vapour was below detection limit, and hence K_p is undefined.

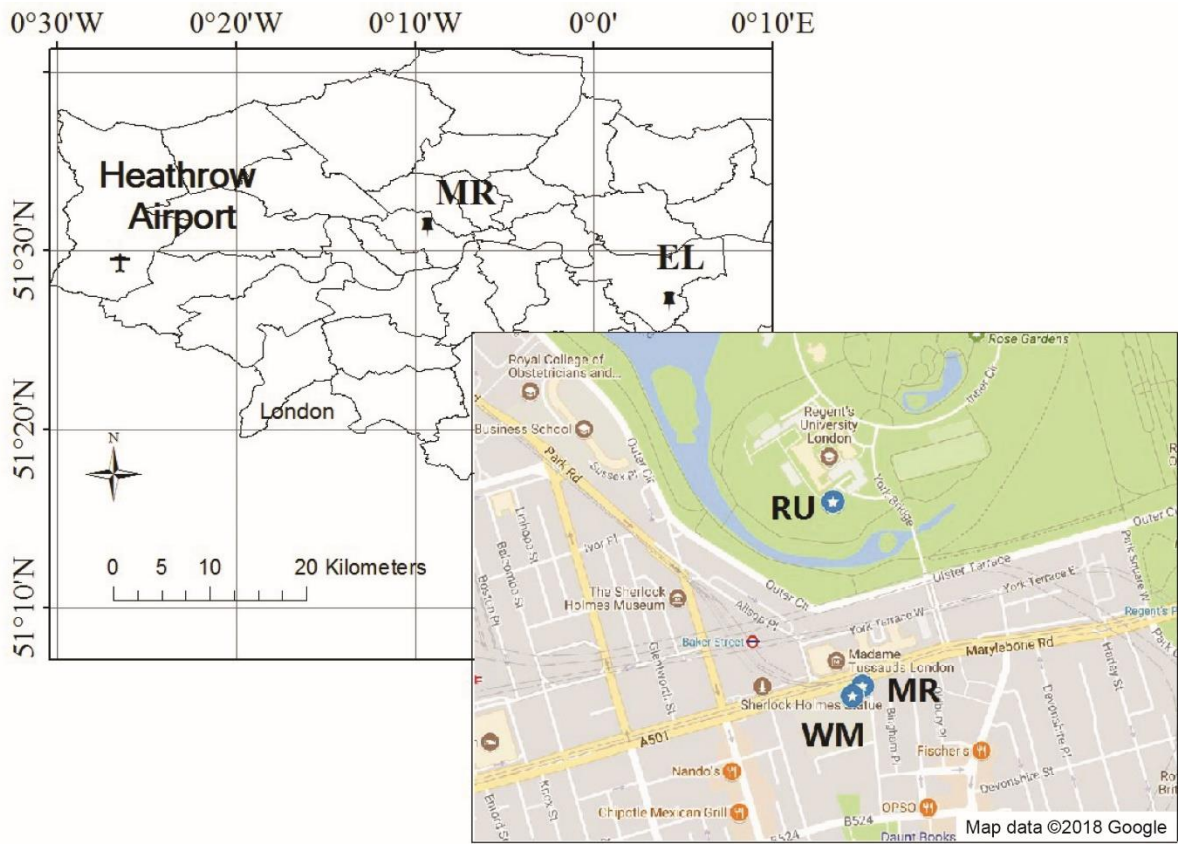


Fig. 1. Map of the sampling sites. RU-Regents University (15 m above ground); WM-University of Westminster (20 m above ground); EL-Eltham; MR-Marylebone Road (south side).

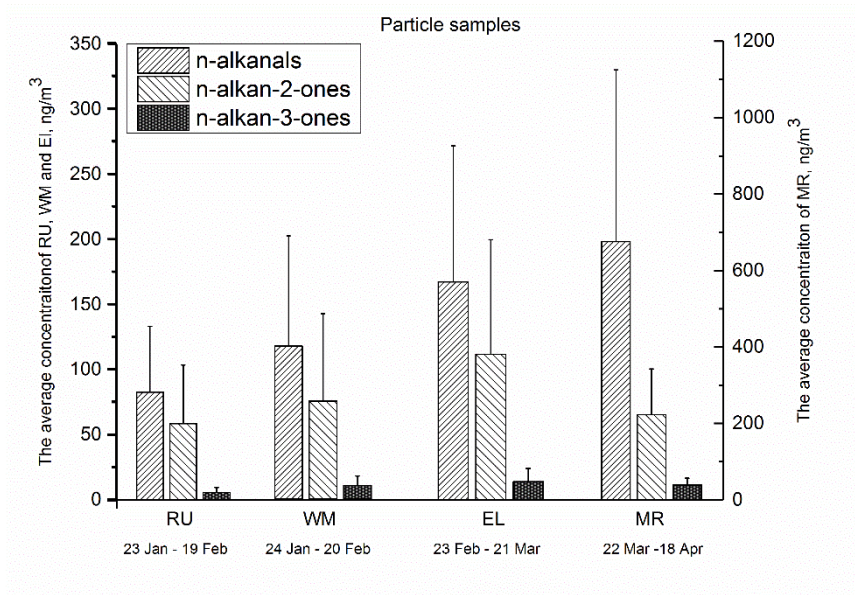


Fig. 2. The average total concentration of particle-bound n-alkanals (C₈-C₂₀), n-alkan-2-ones (C₈-C₂₆), and n-alkan-3-ones (C₈-C₁₉), for each sampling period and site. The error bars indicate one standard deviation.

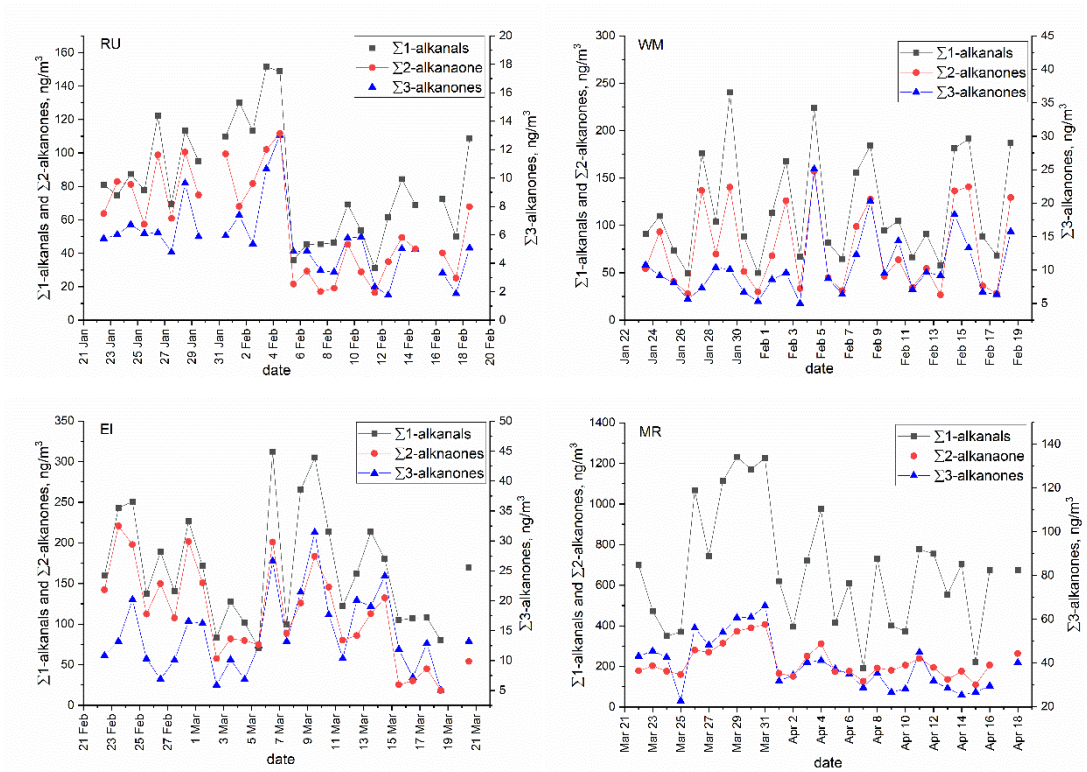


Fig. 3. Time series of particle-bound $\Sigma 1$ -alkanals, $\Sigma 2$ -alkanones and $\Sigma 3$ -alkanones at RU, WM, EL, and MR sites.

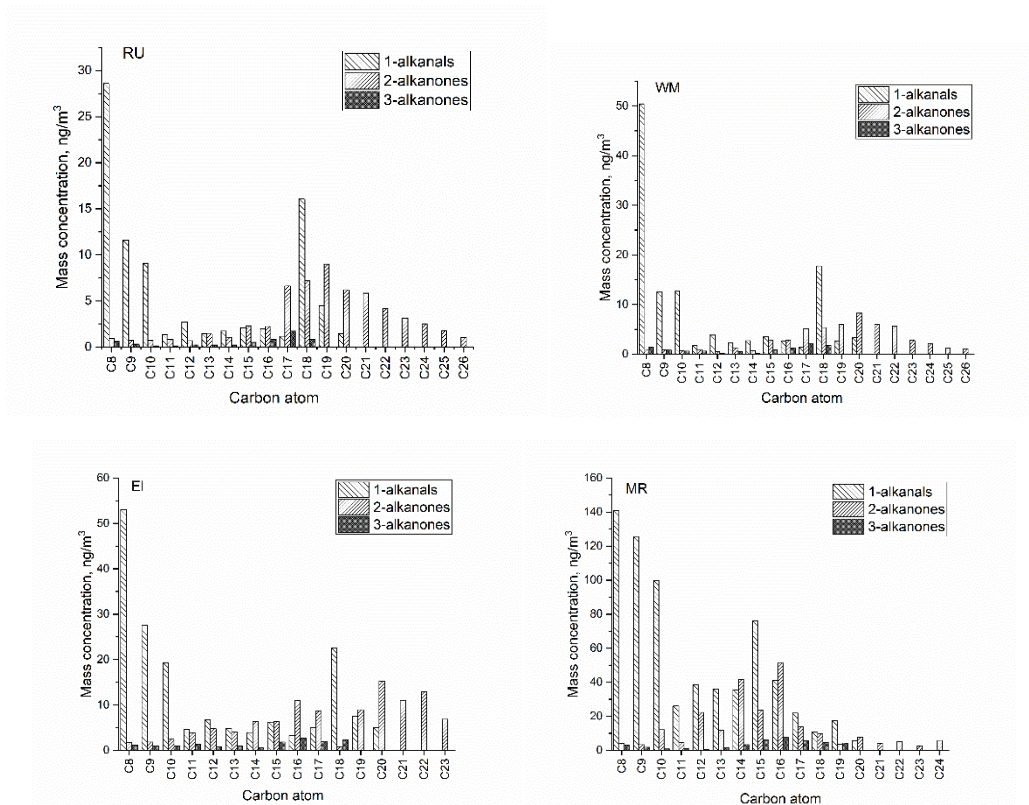


Fig. 4. The molecular distribution of particle-bound carbonyl compounds at four sites (RU, WM, EL, and MR).